Micromechanics modeling of viscoelastic asphalt-filler composite system with and without fatigue cracks

Hui Li [a], Xue Luo [a], Fuquan Ma [a], Yuqing Zhang [b],*

[a] College of Civil Engineering and Architecture, Zhejiang University, 866 Yuhangtang Road, Hangzhou 310058, Zhejiang, China
[b] Department of Civil Engineering, Aston University, Aston Triangle, Birmingham B4 7ET, UK

HIGHLIGHTS

- Shear moduli of asphalt-filler composite systems with filler volumetric contents of 10% and 27% are increased to 1.55 and 3.32 times that of the asphalt binder matrix at 10 Hz, 20℃.
- Viscoelastic strengthening coefficient without fatigue cracks (VSC) decreases with frequency or temperature, and increases with filler volumetric content.
- Viscoelastic strengthening coefficient with fatigue cracks (VSC-f) increases with the filler volumetric content, while decreases rapidly with fatigue crack length.
- VSC and VSC-f of the asphalt-filler composite system are independent of strain level.

GRAPHICAL ABSTRACT
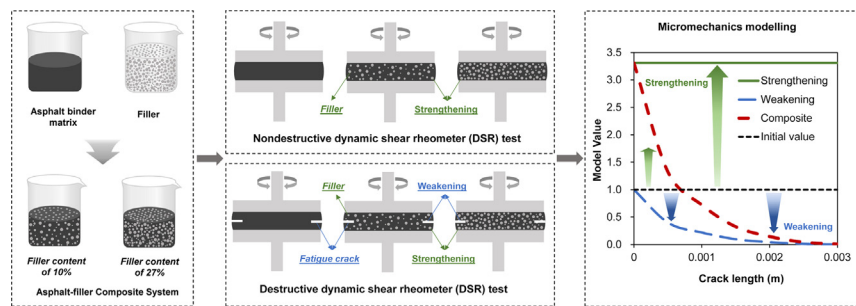
ABSTRACT

Fatigue cracking of viscoelastic asphalt composite materials is one of the major distresses in asphalt pavements. To quantify the weakening effect of the fatigue cracks on the mechanical properties of the viscoelastic asphalt composite materials, this study takes an asphalt-filler composite system as an example, and micromechanics models are proposed by combining Eshbely's equivalent inclusion theory and Mori-Tanaka approach. Dynamic shear rheometer (DSR) tests are performed on the viscoelastic asphalt-filler composite systems with two volumetric contents of inclusion (10% and 27%) at different frequencies (0.1–100 Hz), temperatures (15℃, 20℃, 25℃) and strain levels (0.01%-0.1% for nondestructive DSR tests; 5%, 6%, 7% for destructive DSR tests). Results show that the predicted shear modulus results by a modified viscoelastic strengthening coefficient (VSC) model match with the test results at both low and high filler contents. Then a viscoelastic strengthening coefficient with fatigue cracks (VSC-f) model is proved being capable of accurately predicting the shear modulus for the viscoelastic asphalt-filler composite systems at different strain levels, temperatures, filler contents and damage levels. Both the VSC and the VSC-f model are derived to be dependent of loading frequency, temperature and filler content, but independent of strain level.

© 2021 The Authors. Published by Elsevier Ltd. This is an open access article under the CC BY license (http://creativecommons.org/licenses/by/4.0/).

---

* Corresponding author.
E-mail addresses: huili94@zju.edu.cn (H. Li), xueluo@zju.edu.cn (X. Luo), mafuquan@zju.edu.cn (F. Ma), y.zhang10@aston.ac.uk (Y. Zhang).

1. Introduction

Asphalt materials, such as asphalt mastic, asphalt mortar and asphalt mixture, are widely used in pavement engineering to construct the surface layers of roads, highways, ports, runways and car parks. A large number of studies focused on the behaviors and properties of asphalt materials and pavement structures from the perspective of macroscopic [1–3,52]. However, asphalt materials are typical viscoelastic composite materials, and they are composed of asphalt binder matrix and several heterogeneous inclusions like aggregates, fillers, and air voids. Under the effect of moving vehicles load, the macroscopic mechanical response of the viscoelastic asphalt composite system in pavement structures is effected by the interaction of the asphalt binder matrix and the various inclusions. Currently, a number of analytical models were proposed to predict the macroscopic mechanical properties of viscoelastic asphalt composite system, which can be divided into three categories: (1) Empirical models; (2) Numerical simulation micromodels; (3) Micromechanics models.

In the empirical models, prediction models reflecting the properties of the asphalt binder matrix and aggregate inclusion are usually obtained by regression analysis method. The mechanical properties of the viscoelastic asphalt composite system are predicted based on the mechanical properties of the asphalt binder matrix and aggregate inclusion in the empirical models [4–6]. These empirical models were obtained by statistical regression analysis of test results at specific testing conditions. These empirical models cannot reveal the interacting mechanism caused by the asphalt binder matrix and the inclusions of the viscoelastic asphalt composite system, which limits the development of these empirical models.

For the numerical simulation micromodels, some researchers analyzed the macroscopic mechanical behavior of the viscoelastic asphalt composite system using Finite Element models or Discrete Element models [7–13]. Generally, the complex meso-structure characteristics of the asphalt composite system are introduced into the Finite Element models or Discrete Element models based on the X-ray CT scanning, or the randomized aggregates which are constructed through the image database of the aggregates and the image-assisted random generation method. Then, the Finite Element models and Discrete Element models were solved numerically to predict the macroscale material properties [14–16]. However, analysis of the complex Finite Element models and Discrete Element models requires a number of debugging and large-scale computational costs.

In the micromechanics model, Eshelby proposed the elastic solutions to the stress and strain fields of an elastic infinite medium containing a single inclusion [17–18]. This groundbreaking work provided a solid theoretical foundation for the later micromechanics model of composite materials. Then, on the basis of Eshelby's research, a large number of classical micromechanics models were proposed to predict the macroscopic mechanical properties of composite materials, which including the self-consistent model [19], generalized self-consistent model [20] and Mori-Tanaka model [21], differential model [22–23], J-C model [24], and so on. These models can be used to evaluate the local stress and strain fields of composite materials under given macroscopic loading conditions and to predict the effective mechanical properties of composite materials from the basic mechanical properties of each component. These physically-significant micromechanics models are also widely used in viscoelastic asphalt composite materials [25–27].

The micromechanics models can overcome the limitations of empirical models and do not require large amounts of computational costs, and they can provide reliable estimations of the mechanical properties for the asphalt composite materials. However, most of these models are limited to predict the mechanical properties of the viscoelastic asphalt composite system under a nondestructive condition. The prediction of the mechanical properties is still lack of research for of the viscoelastic asphalt composite system under a destructive condition, for example, a fatigue crack propagation condition. Therefore, it is necessary to extend the micromechanics model to the destructive condition such as fatigue crack propagation when studying the macroscopic mechanical properties for viscoelastic asphalt composite materials.

Asphalt mastic is a typical viscoelastic asphalt-filler composite system which contains the mineral filler particle inclusion and the viscoelastic asphalt binder matrix. Asphalt mastic is an important component of asphalt mixtures, and plays a role of coating and bonding the coarse aggregates in the asphalt mixtures. In this study, the asphalt mastic is taken as an example of the viscoelastic asphalt composite system and the objective of this study is to investigate the influence of fatigue cracks on the mechanical properties of the viscoelastic asphalt-filler composite system and provide a theoretical support for the selection of asphalt materials.

This study is organized as follows. First, materials and laboratory tests are introduced. Then, constitutive equations for the asphalt binder matrix and the filler are presented, and micromechanics models are introduced for the viscoelastic asphalt-filler composite system. Next, a viscoelastic strengthening coefficient (VSC) model is determined for the viscoelastic asphalt-filler composite system under the nondestructive condition. Based on the micromechanics theory, a viscoelastic strengthening coefficient with fatigue cracks (VSC-f) model is derived for the viscoelastic asphalt-filler composite system, which coupled the reinforcement of filler inclusion and the weakening of fatigue crack inclusion under destructive condition. Furthermore, the VSC-f model coupled with temperature, filler content and damage degree are established and verified. Finally, a summary section concludes this study with the main results.

2. Materials and laboratory tests

2.1. Materials

In this study, a type of asphalt binder (AB) and two types of asphalt mastic (AM1 and AM2) with different contents of mineral powder filler were selected as the viscoelastic materials for analysis. Notably, the AB was used as a viscoelastic matrix material, AM1 and AM2 were used as two viscoelastic composite materials with different filler contents where AM1 had a low filler content of 10% and AM2 had a high filler content of 27%. The volumetric content of 27% (i.e., the mass ratio between the powder filler and asphalt binders is 1.0) correspond to the typical ratio of the powder filler to the asphalt binders in the asphalt mixture composition. This volumetric content can be estimated by the gradation information of the mixture, densities of the asphalt binder matrix and filler inclusion. The volumetric content of 10% (i.e., the mass ratio of between the powder filler and the asphalt binder is 0.3) was used to evaluate the applicability of the micromechanical model at different filler contents.

A virgin asphalt binder from Shell was used as the asphalt binder matrix material. Basic properties of the virgin asphalt binder are shown in Table 1, which meet technical requirements of the national specification [28]. In particular, the wax content tests using DSC method were performed on the asphalt binders, and the wax content of the asphalt binders is 0.584%. A limestone from Hubei Province, China was selected as the mineral filler and its material properties were tested and checked against the national specification [28], shown in Table 1. The fabrication of the asphalt-filler viscoelastic composite system included the following

Table 1
Basic properties and requirements of the asphalt binder matrix and filler.

Materials	Sources	Properties	Units	Requirements	Results
Asphalt binder	Shell	Penetration at 25℃	0.1 mm	60–80	66
		Softening point	℃	>=46	49.0
		Ductility at 15℃	cm	>=100	>100
		Wax content	–	–	0.584%
Filler	Hubei Province, China	Relative density	g/cm^3	>=2.50	2.765
		Water content	%	<=1	0.49
		Hydrophilic coefficient	–	<1	0.68

steps: (1) dry the filler in an oven at a temperature of 110℃ for 4 h, and heat the asphalt binder to 145℃ before adding the filler; (2) blend the prepared hot asphalt binder by a high-speed shear dispersion instrument at a rotation speed of 1500 rotations per minute; (3) add the weighed filler according to the designed mixing content to the hot asphalt binder matrix; and (4) mix the filler with the asphalt binder for 10 min to ensure they are fully mixed.

2.2. Laboratory tests

In this study, the DHR-2 of TA instrument was adopted to perform the following series of tests on the AB, AM1 and AM2. It contains frequency sweep test, nondestructive test with different shear strain levels and time sweep test.

2.2.1. Frequency sweep test

To explore the evolution of mechanical properties of the viscoelastic material under different loading frequencies, the frequency sweep tests were conducted on the AB, AM1 and AM2. The shear moduli were obtained to analyze the mechanical correlation between the viscoelastic matrix material (asphalt binder) and the corresponding viscoelastic composite systems (mastics) in frequency domain. Three temperatures were selected for the frequency sweep test in this study, i.e., 15 °C, 20 °C and 25 °C, and the range of frequency domain was 0.1–100 Hz. In addition, a sufficiently small nondestructive strain level of 0.01% was selected as the strain level of the frequency sweep test.

2.2.2. Nondestructive test with different shear strain levels

To explore the evolution of mechanical properties of viscoelastic composite materials under different strain levels, the nondestructive test with different shear strain levels were carried out for the AB, AM1 and AM2. The shear moduli were obtained to analyze the mechanical correlation between viscoelastic matrix material (asphalt binder) and the corresponding viscoelastic composite materials (mastics) at different strain levels. For the nondestructive test with different shear strain levels, three temperatures of 15 °C, 20 °C and 25 °C, one frequency of 10 Hz, and an increasing strain levels within the range of 0.01%-0.1% were selected.

2.2.3. Time sweep test

To establish a micromechanics model for the viscoelastic asphalt-fillers composite system under the destructive condition, it is essential to obtain destructive results of the AB, AM1 and AM2. Hence, the destructive time sweep tests were performed on the AB, AM1 and AM2. Three testing temperatures (15 °C, 20 °C, 25 °C) and one loading frequency (10 Hz) were used. To ensure that the time sweep tests are destructive, relatively high strain levels of 5%, 6% and 7% were applied to the AB, AM1 and AM2. Specific conditions of the frequency sweep test, nondestructive test with different shear strain levels and time sweep test are shown in Table 2.

3. Micromechanics model for viscoelastic asphalt-filler composite system

This section aims to reveal the correlation between the viscoelastic binder matrix, the mineral filler inclusion and the viscoelastic asphalt-filler composite system from the perspective of micromechanics. It mainly consists of the following two parts:

(1) Construct the constitutive equations for the asphalt binder matrix and the filler in Laplace domain;
(2) Introduce the micromechanics theory for the viscoelastic asphalt-filler composite system in the Laplace domain.

3.1. Constitutive equation for the asphalt binder matrix and filler in the Laplace domain

The asphalt binder is a typical viscoelastic material, and its linear viscoelastic constitutive equation can be expressed as follows:

$$\sigma_{ij}^0 = \int_0^t C_{ijkl}^0(t-\tau)\frac{\partial \varepsilon_{kl}^0}{\partial \tau}d\tau \tag{1}$$

where σ_{ij}^0, ε_{kl}^0 are stress tensor and strain tensor of the asphalt binder matrix, respectively; C_{ijkl}^0 is relaxation modulus tensor of the asphalt binder matrix; t is time, and τ is an arbitrary time between 0 and t. The relaxation modulus tensor can be expressed by:

$$C_{ijkl}^0 = \lambda^0 \delta_{ij}\delta_{kl} + G^0\left(\delta_{ik}\delta_{jl} + \delta_{il}\delta_{jk}\right) \tag{2}$$

in which δ_{ij} is *Kronecker* symbol; λ^0, G^0 are *Lame* constant and shear modulus of the asphalt binder matrix. Substituting Eqn 2 into Eqn 1, yields:

$$\sigma_{ij}^0 = \delta_{ij}\int_0^t \lambda^0(t-\tau)\frac{\partial \varepsilon_{kk}^0(t)}{\partial \tau}d\tau + 2\int_0^t G^0(t-\tau)\frac{\partial \varepsilon_{ij}^0(t)}{\partial \tau}d\tau \tag{3}$$

Taking Laplace transformation on Eqn 3, the constitutive equation of the asphalt binder matrix in Laplace domain is obtained as:

$$\bar{\sigma}_{ij}^0(s) = s\bar{\lambda}^0(s)\bar{\varepsilon}_{kk}^0(s)\delta_{ij} + 2s\bar{G}^0(s)\bar{\varepsilon}_{ij}^0(s) \tag{4}$$

where s is Laplace parameter; $\bar{\sigma}_{ij}^0(s)$, $\bar{\varepsilon}_{kk}^0(s)$, $\bar{\varepsilon}_{ij}^0(s)$, $\bar{\lambda}^0(s)$ and $\bar{G}^0(s)$ are stress tensor, volumetric strain tensor, deviatoric strain tensor, Lame constant and shear modulus of the asphalt binder matrix in Laplace domain. In this study, the variables with superscript horizontal lines represent the Laplace transformed variable of the corresponding variables in the time domain.

It is assumed that the filler embedded in the asphalt binder matrix is an isotropic linear elastic material, and the linear elastic constitutive equation can be expressed as follows:

$$\sigma_{ij}^l = \lambda^l \varepsilon_{kk}^l \delta_{ij} + 2G^l \varepsilon_{ij}^l \tag{5}$$

in which σ_{ij}^l, ε_{kk}^l, ε_{ij}^l are stress tensor, volumetric strain tensor and deviatoric strain tensor of the filler; λ^l, G^l are Lame constant and shear modulus of the filler.

Table 2
Schedule of laboratory tests.

Test type	Materials[*]	Temperature (°C)	Frequency (Hz)	Nondestructive strain level	Destructive strain level
Frequency sweep test	AB, AM1, AM2	15	0.1–100	0.01%	–
		20	0.1–100	0.01%	–
		25	0.1–100	0.01%	–
Nondestructive test with different shear strain levels	AB, AM1, AM2	15	10	0.01–0.1%	–
		20	10	0.01–0.1%	–
		25	10	0.01–0.1%	–
Time sweep test	AB, AM1, AM2	15	10	–	5%, 6%, 7%
		20	10	–	5%, 6%, 7%
		25	10	–	5%, 6%, 7%

[*] AB = Asphalt binder; AM1 = Asphalt mastic with filler content of 10%; AM2 = Asphalt mastic with filler content of 27%.

Based on Eqn 4 and 5 of the asphalt binder matrix and filler particle, it can be seen that the constitutive equation of the asphalt binder matrix has the same form as that of the filler particle, a linear elastic material. Therefore, in the Laplace domain, the micromechanics theory of the composite materials based on linear elastic materials can be used to analyze the viscoelastic asphalt-filler composite system.

3.2. Micromechanics theory for viscoelastic asphalt-filler composite system in the Laplace domain

According to the equivalent inclusion theory, due to the presence of internal heterogeneous inclusion, the strain field in matrix of elastic composites is different from that in uniform non-inclusion matrix. The strain field in an arbitrary elastic matrix can be expressed by the following formula [18]:

$$\varepsilon_{ij}^{me} = \varepsilon_{ij}^{0e} + \varepsilon_{ij}^{d} \tag{6}$$

$$\sigma_{ij}^{me} = \sigma_{ij}^{0e} + \sigma_{ij}^{d} \tag{7}$$

where ε_{ij}^{me}, σ_{ij}^{me} represent strain tensor, stress tensor of the matrix disturbed by inclusion, respectively; ε_{ij}^{0e}, σ_{ij}^{0e} are strain tensor, stress tensor of the uniform non-inclusion matrix; ε_{ij}^{d}, σ_{ij}^{d} are disturbed stress and strain tensors caused by the inclusion.

In addition, the strain and stress field of the elastic inclusion are also different from that of the elastic matrix. Assuming that the stress and strain of the inclusion are different from the matrix, the stress and strain of the inclusion can be expressed by [29]:

$$\varepsilon_{ij}^{ne} = \varepsilon_{ij}^{0e} + \varepsilon_{ij}^{d} + \varepsilon_{ij}' \tag{8}$$

$$\sigma_{ij}^{ne} = \sigma_{ij}^{0e} + \sigma_{ij}^{d} + \sigma_{ij}' \tag{9}$$

in which ε_{ij}^{ne}, σ_{ij}^{ne} are strain tensor and stress tensor of an arbitrary elastic inclusion in the composite materials; ε_{ij}', σ_{ij}' are strain and stress tensor of the difference, respectively.

The mastic material composed of the asphalt binder and filler is a typical viscoelastic composite system, so the above-mentioned equivalent inclusion theory of elastic material cannot be directly adopted. However, according to the analysis in the above section, it can be seen that the constitutive equation of the asphalt binder matrix in the Laplace domain has the same form as that of the linear elastic material. In other words, the viscoelastic constitutive equation can be converted into a new form in the Laplace domain where the format of this new form remains the same as that of the corresponding linear elastic constitutive equation. Thus the equivalent inclusion theory in an elastic format can be used for analysis of viscoelastic composite system in the Laplace domain [30]. Therefore, by substituting Eqn 4 into Eqn 6 and 7, the constitutive equation of the asphalt binder matrix disturbed by the filler inclusion can be obtained:

$$\bar{\sigma}_{ij}^{m} = \bar{\sigma}_{ij}^{0} + \bar{\sigma}_{ij}^{d} = s\bar{\lambda}\left(\bar{\varepsilon}_{kk}^{0} + \bar{\varepsilon}_{kk}^{d}\right)\delta_{ij} + 2s\bar{G}^{0}\left(\bar{\varepsilon}_{ij}^{0} + \bar{\varepsilon}_{ij}^{d}\right) \tag{10}$$

where $\bar{\sigma}_{ij}^{m}$, $\bar{\sigma}_{ij}^{d}$ are stress tensor and disturbed stress tensor of the asphalt binder matrix in the Laplace domain, respectively; $\bar{\varepsilon}_{kk}^{d}$, $\bar{\varepsilon}_{ij}^{d}$ are volumetric disturbed strain tensor, deviatoric disturbed strain tensor, respectively.

Similarly, Eqn 8 and 9 are substituted into Eqn 5, and the constitutive equation of the filler inclusion in the asphalt binder matrix is obtained by performing the Laplace transformation as follows:

$$\bar{\sigma}_{ij}^{n} = \bar{\sigma}_{ij}^{I} + \bar{\sigma}_{ij}^{d} + \bar{\sigma}_{ij}'$$
$$= s\bar{\lambda}^{I}\left(\bar{\varepsilon}_{kk}^{I} + \bar{\varepsilon}_{kk}^{d} + \bar{\varepsilon}_{kk}'\right)\delta_{ij} + 2s\bar{G}^{I}\left(\bar{\varepsilon}_{ij}^{I} + \bar{\varepsilon}_{ij}^{d} + \bar{\varepsilon}_{ij}'\right) \tag{11}$$

where $\bar{\sigma}_{ij}^{n}$, $\bar{\varepsilon}_{kk}'$, $\bar{\varepsilon}_{ij}'$, $\bar{\lambda}^{I}(s)$ and $\bar{G}^{I}(s)$ are stress tensor, volumetric strain tensor and deviatoric strain tensor of the difference, *Lame* constant and shear modulus of the filler in the Laplace domain, respectively.

The filler inclusion is different from the asphalt binder matrix, and belongs to heterogeneous inclusion. If the material properties of the filler in Eqn 11 are replaced by the material properties of the asphalt binder matrix, an eigenstrain will arise [17–18]. Therefore, Eqn 11 can be transformed into:

$$s\bar{\lambda}^{I}\left(\bar{\varepsilon}_{kk}^{0} + \bar{\varepsilon}_{kk}^{d} + \bar{\varepsilon}_{kk}'\right)\delta_{ij} + 2s\bar{G}^{I}\left(\bar{\varepsilon}_{ij}^{0} + \bar{\varepsilon}_{ij}^{d} + \bar{\varepsilon}_{ij}'\right)$$
$$= s\left[\bar{\lambda}^{0}\left(\bar{\varepsilon}_{kk}^{0} + \bar{\varepsilon}_{kk}^{d} + \bar{\varepsilon}_{kk}' - \bar{\varepsilon}_{ij}^{*}\right)\delta_{ij} + 2\bar{G}^{0}\left(\bar{\varepsilon}_{ij}^{0} + \bar{\varepsilon}_{ij}^{d} + \bar{\varepsilon}_{ij}' - \bar{\varepsilon}_{ij}^{*}\right)\right] \tag{12}$$

in which $\bar{\varepsilon}_{ij}^{*}$ is the eigenstrain caused by the filler inclusion in the Laplace domain.

According to the Eshelby inclusion theory, there is the following relationship between $\bar{\varepsilon}_{ij}'$ and $\bar{\varepsilon}_{kl}^{*}$ [17]:

$$\bar{\varepsilon}_{ij}' = S_{ijkl}\bar{\varepsilon}_{kl}^{*} \tag{13}$$

in which S_{ijkl} is the Eshelby tensor related to the shape of inclusion and the Poisson's ratio of matrix.

Besides, according to the concept of average stress of Mori-Tanaka approach [29], the disturbed strain $\bar{\varepsilon}_{ij}^{d}$ caused by the filler inclusion can be expressed by the eigenstrain $\bar{\varepsilon}_{kl}^{*}$ as below:

$$\bar{\varepsilon}_{ij}^{d} = -v_{1}\left(S_{ijkl} - I_{ijkl}\right)\bar{\varepsilon}_{kl}^{*} \tag{14}$$

where v_{1} is the volumetric content of the inclusion (i.e., filler) in the viscoelastic asphalt-filler composite system; I_{ijkl} is a unit fourth order tensor.

Eqn 12, 13 and 14 can be solved simultaneously:

$$\bar{G}^l\left(\bar{\varepsilon}_{ij}^l - v_1\left(S_{ijkl} - I_{ijkl}\right)\bar{\varepsilon}_{kl}^* + S_{ijkl}\bar{\varepsilon}_{kl}^*\right)$$
$$= \bar{G}^0\left(\bar{\varepsilon}_{ij}^0 - v_1\left(S_{ijkl} - I_{ijkl}\right)\bar{\varepsilon}_{kl}^* + S_{ijkl}\bar{\varepsilon}_{kl}^* - \bar{\varepsilon}_{ij}^*\right) \tag{15}$$

Substituting the volumetric content for the asphalt binder matrix $v_0 = 1 - v_1$ into Eqn 15, the eigenstrain strain in the Laplace domain can be determined:

$$\bar{\varepsilon}_{ij}^* = \left[\bar{G}^0 - \bar{G}^l\right]\left[\left(\bar{G}^l - \bar{G}^0\right)\left(v_0 S_{ijkl} + V_1 I_{ijkl}\right) - \bar{G}^0\right]^{-1}\bar{\varepsilon}_{ij}^0 \tag{16}$$

In this study, it is assumed that the shear modulus of the filler is much larger than that of the asphalt binder matrix, i.e.,$\bar{\lambda}^0 \ll \bar{\lambda}^l$, $\bar{G}^0 \ll \bar{G}^l$, therefore, Eqn 16 can be simplified as below:

$$\bar{\varepsilon}_{ij}^* = -\left(v_0 S_{ijkl} + v_1 I_{ijkl}\right)^{-1}\bar{\varepsilon}_{kl}^0 \tag{17}$$

Finally, based on the average theory of composite materials, the statistically uniform stress field and strain field can be determined as [30]:

$$\left\langle \bar{\sigma}_{ij} \right\rangle = \frac{1}{V}\iiint_V \bar{\sigma}_{ij}dV \tag{18}$$

$$\left\langle \bar{\varepsilon}_{ij} \right\rangle = \frac{1}{V}\iiint_V \bar{\varepsilon}_{ij}dV \tag{19}$$

in which $\left\langle \bar{\sigma}_{ij} \right\rangle$, $\left\langle \bar{\varepsilon}_{ij} \right\rangle$ are uniform stress and strain of the composite materials in the Laplace domain; V is volume of the composite materials.

In the Laplace domain, both viscoelastic composite materials and linear elastic composite materials have linear constitutive relationship:

$$\left\langle \bar{\sigma}_{ij} \right\rangle = \bar{C}_{ijkl}\left\langle \bar{\varepsilon}_{kl} \right\rangle \tag{20}$$

where $\bar{C}_{ijkl}$ is stiffness matrix of the composite materials in the Laplace domain.

Therefore, by performing the Laplace transformation on the constitutive equations of the asphalt binder matrix, the equivalent inclusion theory for elastic materials will be extended to the viscoelastic composite system. In addition, Huang et, al also introduced the micromechanics theory into the asphalt mixtures [30]. Next, the nondestructive and destructive correlation between the viscoelastic composite system, matrix and inclusion under shear fatigue load will be analyzed, emphatically.

4. Viscoelastic strengthening coefficient for asphalt-filler composite system

To study the correlation between the viscoelastic asphalt-filler composite system, asphalt binder matrix, and inclusion under the destructive shear fatigue load, the influence of the filler inclusion on the asphalt binder matrix must be first formulated under the nondestructive condition. This subsection mainly consists of the following three parts:

(1) Formulate a viscoelastic strengthening coefficient (VSC) model effected by the filler inclusion and asphalt binder matrix;
(2) Determine model parameters of the VSC model based on the viscoelastic Poisson's ratio of the asphalt binder matrix;
(3) Modify the VSC model with high filler content by percolation theory.

4.1. Derivation of viscoelastic strengthening coefficient for asphalt-filler composite system

The viscoelastic asphalt-filler composite system is composed of the asphalt binder matrix and filler inclusion. Comparing with the asphalt binder matrix, the stiffness of the viscoelastic asphalt-filler composite system will be strengthened because of the existence of the rigid filler inclusion. In this subsection, a physical interpretation model representing the enhancement of the filler inclusion will be derived. First, in the Laplace domain, the statistically uniform stress and strain within the viscoelastic asphalt-filler composite system are equal to the corresponding volumetric mean values under the cyclic shear load. Based on Eqn 18, the statistically uniform stress of the viscoelastic asphalt-filler composite system can be calculated as (a detailed derivation is shown in Appendix I):

$$\left\langle \bar{\sigma}_{12}^{eA} \right\rangle = \frac{2}{3}\bar{C}_{1212}^0\bar{\varepsilon}_{12}^0 \tag{21}$$

where $\left\langle \bar{\sigma}_{12}^{eA} \right\rangle$, $\bar{\varepsilon}_{12}^0$, $\bar{C}_{1212}^0$ are statistically uniform apparent stress, apparent shear strain, apparent shear modulus of the viscoelastic asphalt-filler composite system in the Laplace domain, respectively.

Similarly, the statistically uniform strain of the viscoelastic asphalt-filler composite system can be obtained based on Eqn 19, which is present as follows (a detailed derivation is shown in the Appendix I):

$$\left\langle \bar{\varepsilon}_{12}^{eA} \right\rangle = \frac{2}{3}\left[-v_1\left(v_0 S_{1212} + v_1 I_{1212}\right)^{-1} + I_{1212}\right]\bar{\varepsilon}_{12}^0 \tag{22}$$

in which $\left\langle \bar{\varepsilon}_{12}^{eA} \right\rangle$ is statistically uniform apparent shear strain of the viscoelastic asphalt-filler composite system in the Laplace domain.

Dividing Eqn 21 by Eqn 22 and performing the inverse Laplace transformation, the relationship between the viscoelastic asphalt-filler composite system and the asphalt binder matrix is shown:

$$C_{1212}^{eA} = \left[-v_1\left(v_0 S_{1212} + v_1 I_{1212}\right)^{-1} + I_{1212}\right]^{-1}C_{1212}^{0A} = KC_{1212}^{0A} \tag{23}$$

where C_{1212}^{eA}, C_{1212}^{0A} are apparent shear modulus of the viscoelastic asphalt-filler composite system and the asphalt binder matrix, respectively; K is strengthening coefficient, and $K = \left[-v_1\left(v_0 S_{1212} + v_1 I_{1212}\right)^{-1} + I_{1212}\right]^{-1}$.

In this study, the shape of the filler particle inclusion is assumed spherical. Hence, the Eshebly tensor S_{ijkl} is purely related to a Poisson's ratio γ of the asphalt binder matrix, and the Eshebly tensor component S_{1212} can be expressed [29]:

$$S_{1212} = \frac{4 - 5\gamma}{15(1 - \gamma)} \tag{24}$$

Substituting Eqn 24 into K, yields:

$$K = 1 + \frac{15v_1(1 - \gamma)}{v_0(4 - 5\gamma)} \tag{25}$$

Eqn 25 shows that the strengthening coefficient is related to the Poisson's ratio of the asphalt binder matrix and the volumetric content of the filler inclusion, and it increases with the filler inclusion content and the Poisson's ratio of the asphalt binder matrix. Because the stiffness of the filler particle is much larger than that of the asphalt binder matrix, the increase of the filler inclusion content will lead to the enhancement of the asphalt binder matrix. In addition, the smaller the Poisson's ratio of the matrix, the smaller the transverse deformation under the same vertical deformation, i.e., the greater stiffness of the matrix material. If the stiffness of the matrix and filler inclusion remains same, the filler inclusion

will have no strengthening effect on the matrix. If the stiffness of the matrix exceeds the stiffness of the filler inclusion, the filler inclusion will weaken stiffness of the matrix material. In sum, the larger the Poisson's ratio of the matrix, the stronger the reinforcement caused by the filler inclusion.

For the above analysis, one can conclude that the Poisson's ratio of the matrix is particularly important for the enhancement of inclusion, which needs to be accurately characterized. The asphalt binder matrix is particularly sensitive to the temperature and frequency. Therefore, the Poisson's ratio of the asphalt binder matrix is also closely affected by temperature and frequency. To calculate the strengthening coefficient accurately, the Poisson's ratio of the asphalt binder matrix is formulated as a viscoelastic variable that is a function of temperature and frequency. To obtain the viscoelastic strengthening coefficient (VSC), the Carson transformations is performed for Eq. (25), which yields:

$$s \bar{K}(s) = 1 + \frac{15 v_1 \left(1 - s \bar{\gamma}(s)\right)}{v_0 \left(4 - 5s \bar{\gamma}(s)\right)} \tag{26}$$

where $\bar{K}(s)$, $\bar{\gamma}(s)$ are the Laplace transformations of the strengthening coefficient of the viscoelastic asphalt-filler composite system and the Poisson's ratio of the asphalt binder matrix.

So that, the VSC model can be calculated as follows:

$$K^*(\omega) = \left[s \bar{K}(s)\right]_{s=i\omega} = \left[1 + \frac{15 v_1 \left(1 - s \bar{\gamma}(s)\right)}{v_0 \left(4 - 5s \bar{\gamma}(s)\right)}\right]_{s=i\omega} \tag{27}$$

in which ω is loading frequency; and i is an imaginary number.

4.2. Determination of model parameters for viscoelastic strengthening coefficient model

To determine the VSC in Eqn 27, the viscoelastic Poisson's ratio of the asphalt binder matrix must be determined. A time-dependent viscoelastic Poisson's ratio model is adopted for the asphalt binder matrix, which is shown as follows [31]:

$$\gamma(t) = \gamma_0 + \sum_{i=1}^{M} \gamma_i \left(1 - e^{-\frac{t}{q_i}}\right) \tag{28}$$

where $\gamma(t)$ is time-dependent viscoelastic Poisson's ratio of the asphalt binder matrix; γ_0, γ_i and q_i are model parameters; and M is the number of the Maxwell element.

Performing Laplace transformation on Eqn 28 yields:

$$\bar{\gamma}(s) = \frac{\gamma_0}{s} + \sum_{i=1}^{M} \frac{\gamma_i}{s(sq_i + 1)} \tag{29}$$

Substituting Eqn 29 into Eqn 27, a parameterized VSC model can be obtained:

$$K^*(\omega) = \left[s \bar{K}(s)\right]_{s=i\omega} = \left[1 + \frac{15 v_1 \left(1 - s \left(\frac{\gamma_0}{s} + \sum_{i=1}^{M} \frac{\gamma_i}{s(sq_i+1)}\right)\right)}{v_0 \left(4 - 5s \left(\frac{\gamma_0}{s} + \sum_{i=1}^{M} \frac{\gamma_i}{s(sq_i+1)}\right)\right)}\right]_{s=i\omega} \tag{30}$$

Eqn 30 shows $K^*(\omega)$ is a complex number, the real part and the imaginary part of $K^*(\omega)$ can be separated as:

$$K'(\omega) = 1 + \frac{3 v_1}{v_0}$$
$$+ \frac{3 v_1 \left(4 - 5\gamma_0 - 5\sum_{i=1}^{M} \frac{\gamma_i}{(\omega^2 q_i^2 + 1)}\right)}{v_0 \left(\left(4 - 5\gamma_0 - 5\sum_{i=1}^{M} \frac{\gamma_i}{(\omega^2 q_i^2 + 1)}\right)^2 + \left(\sum_{i=1}^{M} \frac{5q_i\gamma_i\omega}{(\omega^2 q_i^2 + 1)}\right)^2\right)} \tag{31}$$

$$K''(\omega) = \frac{-3 v_1 \left(\sum_{i=1}^{M} \frac{5q_i\gamma_i\omega}{(\omega^2 q_i^2 + 1)}\right)}{v_0 \left(\left(4 - 5\gamma_0 - 5\sum_{i=1}^{M} \frac{\gamma_i}{(\omega^2 q_i^2 + 1)}\right)^2 + \left(\sum_{i=1}^{M} \frac{5q_i\gamma_i\omega}{(\omega^2 q_i^2 + 1)}\right)^2\right)} \tag{32}$$

Hence, the magnitude of the VSC is $|K^*(\omega)| = \sqrt{K'(\omega)^2 + K''(\omega)^2}$. To determine the VSC in Eqn 31 and 32, the model parameters γ_0, γ_i and q_i of the viscoelastic Poisson's ratio are needed. Below will explain how these model parameters will be determined from the complex Poisson's ratio.

First, the complex Poisson's ratio of the asphalt binder matrix can be calculated by the following expression [32]:

$$|\gamma^*(\omega)| = \gamma_{00} + (\gamma_0 - \gamma_{00}) \frac{|G^*(\omega)| - G_{00}}{G_0 - G_{00}} \tag{33}$$

in which γ_{00}, γ_0, G_{00} and G_0 are model parameters; $|G^*(\omega)|$ is the magnitude of the frequency-dependent complex modulus which are measured by the frequency sweep tests. Besides, the values of the model parameters (in Eqn 33) can be found in the study [32].

Second, the shear modulus of the asphalt binder matrix at different temperatures and frequencies can be obtained by performing the nondestructive frequency sweep test. Then the master curve of the complex Poisson's ratio is modeled by a sigmoidal function [33]:

$$|\gamma^*(\omega)| = \delta + \frac{\kappa}{1 + \eta \exp[\lambda - \beta \log(\alpha_T)]} \tag{34}$$

where $\kappa, \delta, \eta, \beta$ are model parameters of the sigmoidal function of the complex Poisson's ratio; α_T is time–temperature shifted factor modelled by the WLF function, and $\log(\alpha_T) = -\frac{C_1(T - T_{ref})}{C_2 + T - T_{ref}}$; C_1, C_2 are model parameters of the shift factor; T, T_{ref} are absolute temperature and reference temperature, respectively. These model parameters of the mastic curve of the complex Poisson's ratio of the asphalt binder matrix are shown in Table 3.

Fig. 1 shows measured complex Poisson's ratio at 15℃, 20℃, 25℃ and constructed master curve of the complex Poisson's ratio at 20℃ for the asphalt binder matrix. Fig. 1 shows that the complex Poisson's ratio of asphalt binder matrix decreases with the increase of the frequency, while it increases with the temperature. Moreover, the complex Poisson's ratio is close to 0.5 at a high temperature or a low frequency. This is because the asphalt binder matrix exhibits fluidic behavior at the high temperature or the low frequency.

Third, a theoretical relation shown in Eqn 35 exists between the complex Poisson's ratio model and the time-dependent viscoelastic Poisson's ratio model [34]:

$$|\gamma^*(\omega)| = \sqrt{\left[\gamma_0 + \sum_{i=1}^{M} \gamma_i - \sum_{i=1}^{M} \frac{\omega^2 q_i^2 \gamma_i}{1 + \omega^2 q_i^2}\right]^2 + \left[\sum_{i=1}^{M} \frac{\omega q_i \gamma_i}{1 + \omega^2 q_i^2}\right]^2} \tag{35}$$

Using the master curve data from Eqn 34 and 35, the model parameters (γ_0, γ_i and q_i) of the time-dependent viscoelastic Poisson's ratio model can be determined by the "Solver" function in Microsoft Excel, as shown in Table 4.

Finally, the VSC model can be obtained by substituting γ_i and q_i from Table 3 into Eqn 31 and 32. Fig. 2 presents evolution of the VSC with frequency at 15℃, 20℃, 25℃ and the master curve of the VSC for the AM1. The evolution trend of the VSC is similar to that of the complex Poisson's ratio. It can be seen that the VSC increases with the increase of the frequency, because the asphalt material is closer to the elastic solid under high frequencies, while it is closer to the fluid under low frequencies. It can be predicted

Table 3
Model parameters of the master curve and shift model.

Model parameters	C_1	C_2	κ	β	η	δ	λ
Complex Poisson's ratio	7.630	79.059	0.500	0.0031	−1.240	0.0001	0.185
Viscoelastic strength coefficient (VSC) model (asphalt mastic with filler content of 10%)	7.654	79.566	1.554	0.0007	−1.172	0.0022	0.114
Viscoelastic strength coefficient (VSC) model (asphalt mastic with filler content of 27%)	7.654	79.566	3.337	0.0015	−1.130	0.0042	0.122
Viscoelastic strengthening coefficient with fatigue cracks (VSC-f) model	0.025	1.796	0.736	3.87E9	3.999	–	–
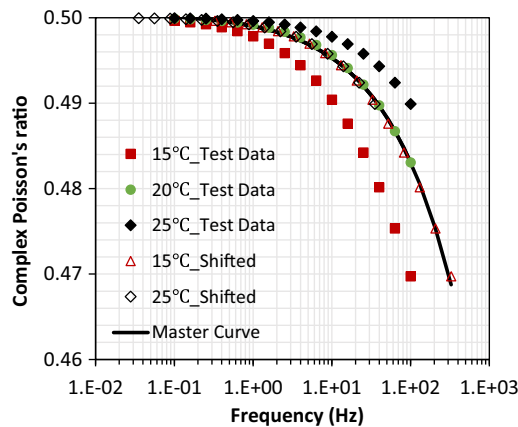
Fig. 1. Complex Poisson's ratio at 15℃, 20℃, 25℃ and the constructed master curve at 20℃ for the asphalt binder matrix.
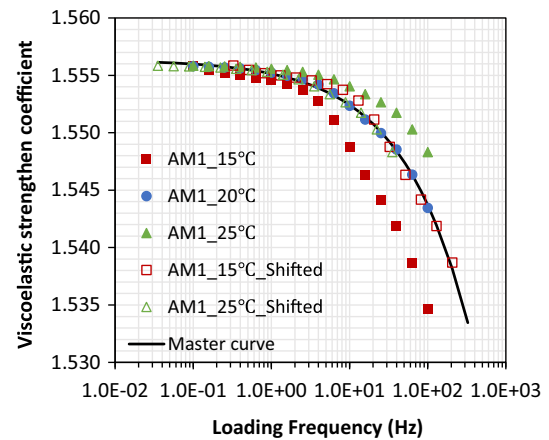
Fig. 2. Viscoelastic strength coefficient at 15℃, 20℃, 25℃ and the master curve of the strength coefficient for the AM1 (AM1 = asphalt mastic with filler content of 10%).

that when the asphalt binder matrix is soft, the enhancement effect of the filler to the asphalt binder matrix is relatively higher compared to that when the asphalt binder matrix is stiff. In this study, to obtain the VSC model coupled with frequency and temperature, the sigmoidal function is used to formulate the mastic curve model for the VSC at different temperatures, which is expressed as below:

$$|K^*(\omega)| = \delta_k + \frac{\kappa_k}{1 + \eta_k \exp[\lambda_k - \beta_k \log(\alpha_T)]} \qquad (36)$$

where δ_k, κ_k, η_k, β_k are VSC model parameters; and α_T is the same time–temperature shifted factor as the complex Poisson's ratio.

Fig. 2 presents that calculated results have an agreement with the sigmoidal function, and model parameters of the mastic curve of the VSC are shown in Table 3. Furthermore, the VSC is multiplied by the shear modulus of the asphalt binder matrix to obtain the predicted shear modulus of the viscoelastic asphalt-filler composite system at different frequencies, temperatures, and strain levels. Fig. 3 compares tested shear modulus and predicted shear modulus modulus of the AM1 at different frequencies, temperatures and strain levels. It can be seen that the predicted results by the VSC model match with the test results for the AM1. Fig. 3a shows that shear modulus of the AM1 increases with the increase of the fre-

quency or the decrease of the temperature. Fig. 3b presents that shear modulus of the AM1 remains unchanged when the strain level increases. This is because the strain levels used in the nondestructive test are small and the asphalt material is in an undamaged condition at these strain levels. It is found that the VSC model can predict the shear modulus of the composite materials at different strain levels, thus it is independent of the strain level.

4.3. Modified viscoelastic strengthening coefficient at a high filler content

By substituting the filler volumetric content into Eqn 31 and 32, the VSC with high filler content (e.g., AM2 with filler content of 27%) can be obtained. Predicted shear modulus can be obtained by multiplying the VSC by the shear modulus of the asphalt binder matrix. Fig. 4a compares the predicted and measured shear modulus of the AM2 at different temperatures. It is indicated that the predicted shear moduli are smaller than the experimental results. This is because the Eshelby tensor is established for a single inclusion embedded in an infinite matrix based on the concept of Mori-Tanaka equivalent principle, which is true only when the inclusion

Table 4
Model parameters of the time-dependent viscoelastic Poisson's ratio of the asphalt binder matrix.

Model parameters	Temperature (℃)				Relaxation time (s)	
	15	20	25			
γ_0	0.43852	0.45610	0.45757			
γ_1	0.00679	0.00681	0.01307		q_1	0.00001
γ_2	0.00389	0.00417	0.00655		q_2	0.0001
γ_3	0.00594	0.00636	0.00649		q_3	0.001
γ_4	0.02845	0.01898	0.01237		q_4	0.01
γ_5	0.01393	0.00618	0.00334		q_5	0.1
γ_6	0.00091	0.00119	0.00052		q_6	1
γ_7	0.00219	0.00010	0.00005		q_7	10
γ_8	0.00689	0.00537	0.00081		q_8	100
γ_9	0.29113	0.28449	0.13996		q_9	1000
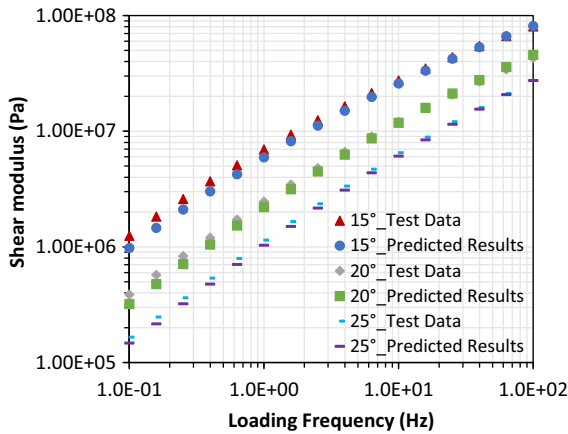
a. Measured shear modulus vs. predicted shear modulus of the AM1 at different loading frequencies and temperatures
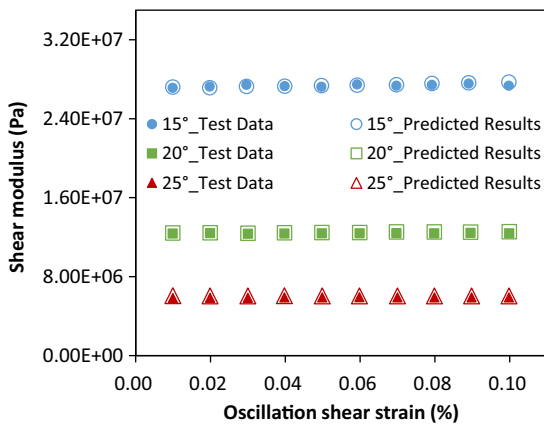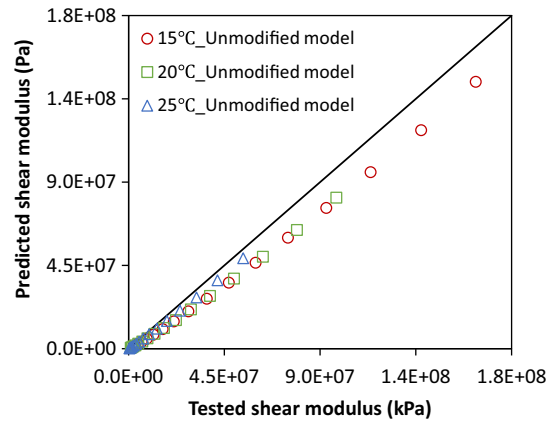

b. Measured shear modulus vs. predicted shear modulus of the AM1 at different strain levels

Fig. 3. Measured shear modulus vs. predicted shear modulus of the AM1 (AM1 = asphalt mastic with filler content of 10%) at different loading frequencies, temperatures and strain levels.
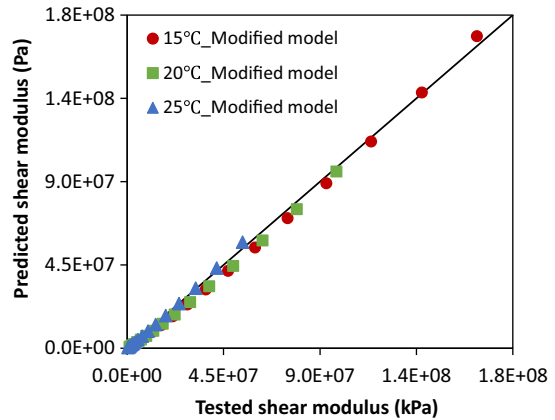

a.Predicted shear modulus by unmodified VSC model and tested shear modulus of the AM2 at different temperatures

b.Predicted shear modulus by modified VSC model and tested shear modulus of the AM2 at different temperatures

Fig. 4. Comparison among the predicted shear modulus by unmodified VSC model, the modified VSC model and tested shear modulus of the AM2 (AM2 = asphalt mastic with filler content of 27%) at different temperatures (VSC = Viscoelastic strength coefficient).

content is low. However, the matrix surrounding each particle inclusion is not an infinite matrix due to the relatively high inclusion content for the AM2.

In view of this deviation, the VSC is modified by percolation theory in this study. The percolation theory shows that when the volumetric content of the inclusion is low, the distribution of inclusions in the matrix is random and these inclusions do not affect each other, thus, the matrix materials are continuous, which is called percolated phase [35]. When the volumetric content of the inclusions is high, the probability of interactions among inclusions increases. Therefore, when the filler content is high, the distribution of the inclusions in the matrix are not random and some of the matrix are completely wrapped by the filler particles. The asphalt binder matrix wrapped by the filler combines with the surrounding filler particles and forms a larger inclusion. In this case, an effective matrix volumetric content is smaller than a true matrix volumetric content, while the effective inclusion volumetric content is larger than the true inclusion volumetric content.

Research has shown that when the inclusion volumetric content exceeds 20% (a critical volumetric content is denoted as ϕ_{fpt}), the damping factor of the composite materials decreases sharply [36]. In addition, an upper limit volumetric content is related to the gradation of the inclusion (the upper limit volumetric content $\phi_{f\max} = 1 - 0.47(d/D)^{0.2}$, where d and D represent the minimum

and maximum particle sizes of the inclusion, respectively [35]). Furthermore, when the volumetric content of the matrix ϕ_m has the relationship $(1 - \phi_{f\max}) < \phi_m < \phi_{fpt}$, the effective inclusion volumetric content can be calculated by [37]:

$$\phi_{eff} = 1 - \left(1 - \phi_f\right)\left(\frac{1 - \phi_f/\phi_{f\max}}{1 - \phi_{fpt}/\phi_{f\max}}\right)^{0.4} \qquad (37)$$

Substituting the parameters ϕ_f, $\phi_{f\max}$, ϕ_{fpt} into Eqn 37, the effective inclusion volumetric content can be determined $\phi_f = \min\{\phi_{f\max}, \phi_{eff}\} = 31.8\%$. Then, substituting the effective inclusion volumetric content into the Eqn 31 and 32, the modified effective inclusion volumetric content with high inclusion content can be obtained.

Fig. 4b compares the shear modulus predicted by the modified VSC model with the measured shear modulus of the AM2 at different temperatures. It is demonstrated that the predicted shear modulus from the modified VSC model match with the experimental results. In addition, Fig. 5 presents the evolution of the modified VSC at 15℃, 20℃, 25℃ and the master curve of the modified VSC for the AM2. It shows that evolution trend is similar to that of the viscoelastic Poisson's ratio. Hence, sigmoidal function is used to establish the mastic curve for the modified VSC of the AM2, and model parameters are shown in Table 3. It can be seen from

Fig. 5 that the sigmoidal function can effectively model the modi-fied VSC.

Fig. 6 shows measured shear modulus and predicted results of the AM2 at different frequencies, temperatures and strain levels. It can be seen from Fig. 6a that the predicted results based on the modified VSC and tested data have a good agreement with the measured results at different temperatures and frequencies, and Fig. 6b presents the VSC is independent of strain level. It is indicated that the conclusions obtained in Fig. 3 for low inclusion volumetric content are applicable for that of the high inclusion volumetric content.

5. Viscoelastic strengthening coefficient with fatigue cracks for asphalt-filler composite system

The effects of the asphalt binder matrix and fillers inclusion have been considered in Section 4, but fatigue cracks have not been considered when fatigue cracks exist in the composite system. In this section, the composite system without the fatigue cracks is regarded as the matrix material, and the fatigue cracks are regarded as the inclusions. To formulate the micromechanics model for the asphalt-filler composite system with fatigue cracks, two parts are contained in this subsection:

(1) Derive a viscoelastic strengthening coefficient with fatigue cracks (VSC-f) for the asphalt-filler composite system;
(2) Formulate a VSC-f model coupled with the temperature, filler content, and damage degree under destructive condition.

5.1. Derivation of viscoelastic strengthening coefficient with fatigue cracks for asphalt-filler composite system

In this study, the linear elastic constitutive equation is used to model the fatigue crack, which is shown as below:

$$\sigma_{ij}^{II} = \lambda^{II}\varepsilon_{kk}^{II}\delta_{ij} + 2G^{II}\varepsilon_{ij}^{II} \tag{38}$$

in which σ_{ij}^{II} is stress tensor of the fatigue crack; λ^{II}, G^{II} are *Lame* constant and shear modulus of the fatigue crack.

Taking the Laplace transform for Eqn 38, obtains:

$$\bar{\sigma}_{ij}^{II}(s) = s\bar{\lambda}^{II}(s)\bar{\varepsilon}_{kk}^{II}(s)\delta_{ij} + 2s\bar{G}^{II}(s)\bar{\varepsilon}_{ij}^{II}(s) \tag{39}$$
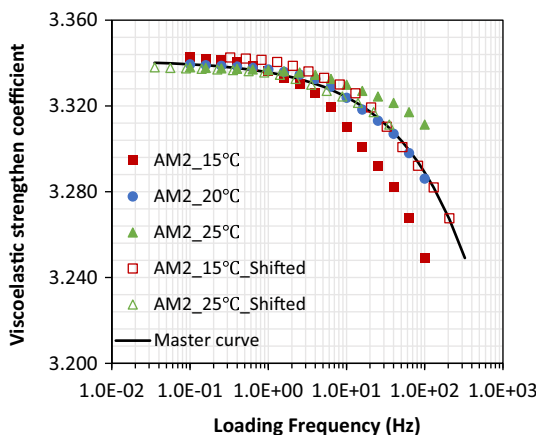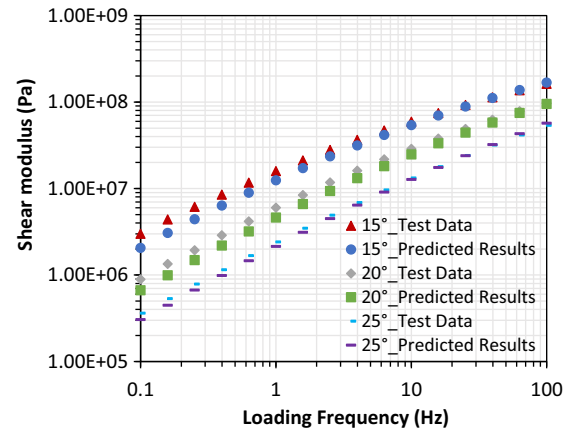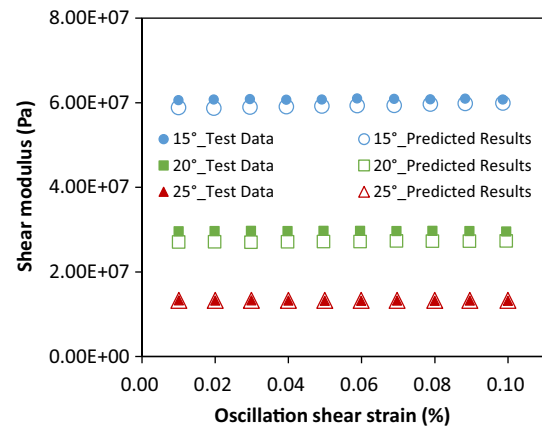

Fig. 5. Evolution of the modified viscoelastic strengthening coefficient with frequency at 15℃, 20℃, 25℃ and master curve of the modified viscoelastic strengthening coefficient for the AM2 (AM2 = asphalt mastic with filler content of 27%).

a. Measured shear modulus vs. predicted shear modulus of the AM2 at different frequencies, temperatures

b. Measured shear modulus vs. predicted shear modulus of the AM2 at different strain levels

Fig. 6. Measured shear modulus vs. predicted shear modulus of the AM2 (AM2 = asphalt mastic with filler content of 27%) at different frequencies, temperatures and strain levels.

For fatigue crack, it is assumed that the fatigue crack is an inclusion embedded in the asphalt-filler composite system, and the inside of the fatigue crack contains gas, whose stiffness is very small and can be regarded as zero. Thus, the mechanical properties of the fatigue crack are also different from the asphalt binder matrix, and it is regarded as heterogeneous inclusion compared with the asphalt binder matrix. The fatigue crack is regarded as a type of inclusion, and the same model as the filler inclusion is adopted. Similarly, in the Laplace domain, stress and strain field of the matrix have the following relationship:

$$\bar{\sigma}_{ij}^{mc} = \bar{\sigma}_{ij}^{m0} + \bar{\sigma}_{ij}^{md} = s\bar{C}_{ijkl}^{mc}\left(\bar{\varepsilon}_{kl}^{m0} + \bar{\varepsilon}_{kl}^{md}\right) \tag{40}$$

where $\bar{\sigma}_{ij}^{mc}$, $\bar{\sigma}_{ij}^{md}$ are stress tensor and disturbed stress tensor of the matrix in the Laplace domain, respectively; $\bar{\varepsilon}_{kk}^{md}$, $\bar{\varepsilon}_{ij}^{md}$ are volumetric disturbed strain tensor, deviatoric disturbed strain tensor in the Laplace domain, respectively; $\bar{C}_{ijkl}^{mc}$ is stiffness tensor of the matrix in the Laplace domain.

Furthermore, the relationship between the stress and strain field of the fatigue crack inclusions can be expressed by:

$$\bar{\sigma}_{ij}^{c} = \bar{\sigma}_{ij}^{m0} + \bar{\sigma}_{ij}^{md} + \bar{\sigma}_{ij}'' = s\bar{C}_{ijkl}^{c}\left(\bar{\varepsilon}_{kl}^{m0} + \bar{\varepsilon}_{kl}^{md} + \bar{\varepsilon}_{kl}''\right) \tag{41}$$

in which $\bar{\sigma}_{ij}^{c}$, $\bar{\sigma}_{ij}''$, $\bar{\varepsilon}_{kl}''$, $\bar{C}_{ijkl}^{c}$ are stress tensor, volumetric stress tensor and deviatoric stress tensor of the difference caused by the fatigue crack inclusions, stiffness tensor of the fatigue crack in the Laplace domain, respectively.

The fatigue crack is heterogeneous inclusion in viscoelastic asphalt-filler composite system. When the strain field of the fatigue crack inclusion is represented by that of the matrix, an eigenstrain $\bar{\varepsilon}_{kl}^{**}$ caused by the fatigue crack inclusion needs to be introduced. The Eqn 41 can be rewritten as below:

$$\bar{\sigma}_{ij}^{c} = \bar{C}_{ijkl}^{c}\left(\bar{\varepsilon}_{kl}^{m0} + \bar{\varepsilon}_{kl}^{md} + \bar{\varepsilon}_{kl}''\right) = \bar{C}_{ijkl}^{mc}\left(\bar{\varepsilon}_{kl}^{m0} + \bar{\varepsilon}_{kl}^{md} + \bar{\varepsilon}_{kl}'' - \bar{\varepsilon}_{kl}^{**}\right) \qquad (42)$$

Similarly, according to the Eshelby inclusion theory, has:

$$\bar{\varepsilon}_{ij}'' = S_{ijkl}^{c}\bar{\varepsilon}_{kl}^{**} \qquad (43)$$

in which S_{ijkl}^{c} is Eshelby tensor caused by the fatigue crack inclusion.

Based on the average stress concept from the Mori-Tanaka approach, the disturbed stress is self-consistent, i.e., the volume average of the disturbed stress should be zero:

$$v_c(\sigma^{md} + \sigma'') + (1 - v_c)\sigma^{md} = 0 \qquad (44)$$

Combining Eqn 40, 41, 42, 43 and 44 can be obtained:

$$\bar{\varepsilon}_{ij}^{md} = v_c\left(I - S_{ijkl}^{c}\right)\bar{\varepsilon}_{kl}^{**} \qquad (45)$$

It is assumed that the fatigue crack has a linear elastic constitutive relationship in this study, however, the inside of the fatigue crack contains gas, whose stiffness is very small and can be ignored. Therefore, the fatigue crack can deform, but there is no internal stress, the following formula holds:

$$\bar{\sigma}_{ij}^{c} = \bar{C}_{ijkl}^{mc}\left(\bar{\varepsilon}_{ij}^{m0} + \bar{\varepsilon}_{ij}^{md} + \bar{\varepsilon}_{ij}'' - \bar{\varepsilon}_{ij}^{**}\right) = 0 \qquad (46)$$

The stiffness matrix $\bar{C}_{ijkl}^{mc}$ in Eqn 46 must not be zero, thus:

$$\bar{\varepsilon}_{ij}^{m0} + \bar{\varepsilon}_{ij}^{md} + \bar{\varepsilon}_{ij}'' - \bar{\varepsilon}_{ij}^{**} = 0 \qquad (47)$$

Solving Eqn 43, 45 and 47 simultaneously, yields:

$$\bar{\varepsilon}_{ij}^{**} = -\frac{1}{1 - v_c}\left(S_{ijkl}^{c} - I\right)^{-1}\bar{\varepsilon}_{kl}^{m0} \qquad (48)$$

When the destructive time sweep test is performed on the viscoelastic asphalt-filler composite system, the following expression can be obtained:

$$\bar{C}_{1212}^{eA} = \bar{\varepsilon}_{12}^{m0}\left(\bar{\varepsilon}_{12}^{m0} + v_c\bar{\varepsilon}_{12}^{**}\right)^{-1}\bar{C}_{1212}^{m0} \qquad (49)$$

Eqn 24 and 48 are substituted into Eqn 49, and performing the inverse Laplace transformation, which yields:

$$C_{1212}^{eA} = \left\{I_{1212} - \frac{v_c}{1 - v_c}\left(S_{1212}^{c} - I_{1212}\right)^{-1}\right\}^{-1} K C_{1212}^{0A} = K_c C_{1212}^{0A} \qquad (50)$$

where K_c is viscoelastic strengthening coefficient of the viscoelastic asphalt-filler composite system under the destructive condition.

It can be found that K_c can be expressed as the product of $\left\{I_{1212} - \frac{v_c}{1 - v_c}\left(S_{1212}^{c} - I_{1212}\right)^{-1}\right\}^{-1}$ and the VSC. Moreover, $\left\{I_{1212} - \frac{v_c}{1 - v_c}\left(S_{1212}^{c} - I_{1212}\right)^{-1}\right\}^{-1}$ contains the fatigue crack volumetric content and Eshelby tensor component of the fatigue crack inclusion. This value is less than one because the fatigue crack inclusion has a weakening effect on the composite materials. In addition, according to the previous analysis, calculated value of the VSC is always greater than one, because the filler inclusion has an enhanced effect on the composite materials.

5.2. Determination of viscoelastic strengthening coefficient with fatigue cracks for asphalt-filler composite system

The variables of the VSC-f of the viscoelastic asphalt-filler composite system contain the fatigue crack volumetric content v_c, the Eshebly tensor S_{1212}^{c} of the fatigue crack and the VSC. The fatigue crack will propagate, fatigue crack volumetric content and morphology affected the VSC-f will change when performing the destructive time sweep test on the viscoelastic asphalt-filler composite system. In addition, the fatigue crack is initiated from the edge of the specimen, then grows toward the sample center to form an edge crack [38–41,50,51]. It is difficult to determine the Eshelby tensor component of the edge crack. Therefore, another method is adopted to obtain the VSC-f model in this section. First, based on Eqn 50, the S_{1212}^{c} can be back-calculated by using the initial shear modulus of the asphalt binder matrix and the shear modulus of the composite system at different crack lengths which are determined using a model developed by author from a previous study [38].

Fig. 7a shows an example of evolution of S_{1212}^{c} with crack length for the viscoelastic asphalt-filler composite system with different filler contents. It presents that S_{1212}^{c} increases with the crack length and S_{1212}^{c} increases with the filler content at the same crack length.
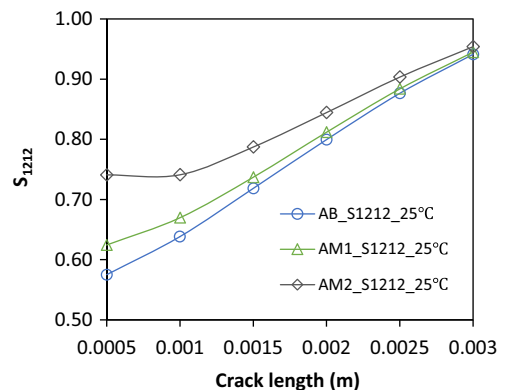
a. Evolution of Eshebly tensor S_{1212}^{c} with the crack length with different filler contents
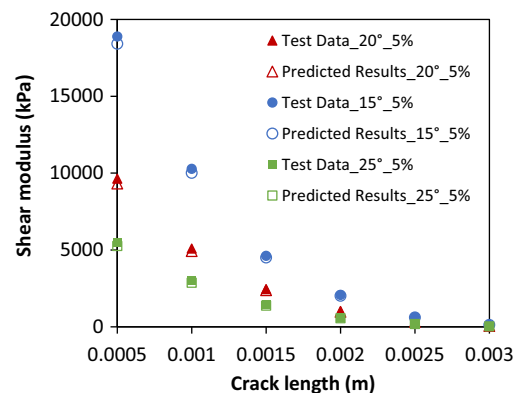

b. Predicted results vs. test data of the shear modulus of AM2 at three temperatures, 5% of strain level

Fig. 7. Eshebly tensor and comparison between predicted results and test data of shear modulus of AM2 (AM2 = asphalt mastic with filler content of 27%).

This is because S_{1212}^c depends on the fatigue crack morphology and Poisson's ratio of the asphalt binder matrix which decreases with the filler content. It is indicated that S_{1212}^c increase with the Poisson's ratio. Besides, Fig. 7b presents an example that comparison between predicted results and test data of the shear modulus of AM2 at three temperatures, 5% of strain level. It can be seen that the predicted results match with the test results. It is showed that the back-calculated Eshelby tensor is valid.

Fig. 8a and b show the VSC-f of the AM1 and AM2 at different temperatures, strain levels and fatigue crack lengths, respectively. It is indicated that the VSC-f decreases with the increase of the fatigue crack length. When the VSC-f is close to zero, the viscoelastic asphalt-filler composite system is near completely damaged. Because the shear modulus of the viscoelastic asphalt-filler composite system decreases rapidly with the fatigue crack, while the fatigue crack cannot bear the load. In addition, the VSC-f of two type of composite materials is unchanged at different strain levels (5%, 6%, 7%) of 15℃ and 25℃. It is showed that the VSC-f is independent of strain level, same as the observations from Fig. 3b and 6b.

To establish the VSC-f model coupled with temperature, filler content and damage degree, a shift factor function should be first modeled. The only difference from the shift factor function of the complex Poisson's ratio is that the term of the filler content is added in this model. Moreover, the VSC-f decreases rapidly with the increase of the crack length which is shown in Fig. 9a.
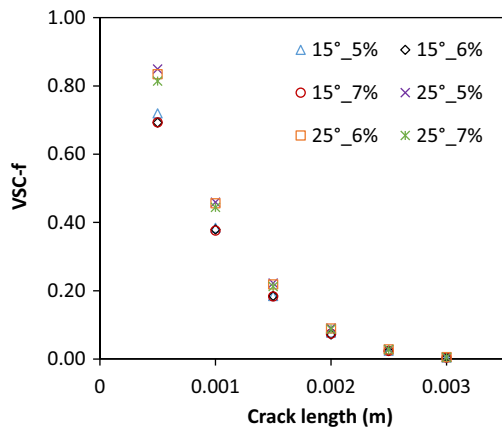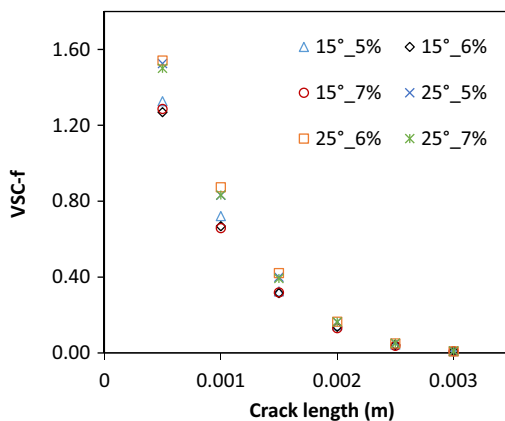
Therefore, the VSC-f model and the corresponding shift factor function adopted are present below:

$$K_c = \beta \left[\alpha_T \left(r^A - c \right) \right]^{\eta} \tag{51}$$

$$\alpha_T = 10^{-\frac{c_1 \left(T - T_{ref} \right)}{c_2 + T - T_{ref}}} + \kappa v_1 \tag{52}$$

where r^A is radius of the specimen; c is crack length of the specimen; κ, β, η are model parameters, and κ contains the effect of the filler content. These model parameters are shown in Table 3.

Fig. 9 presents calculation results and shift model of the VSC-f of the AB, AM1 and AM2 at different temperatures, and a shifted crack length is defined as $c_T = r^A - \alpha_T \left(r^A - c \right)$. Four conclusions can be drawn from Fig. 8a and b: (1) the VSC-f decreases rapidly with the increase of crack length. The reason is that the fatigue crack inclusion weakens the strength of the composite system, and this weakening effect increases with the fatigue crack length; (2) the VSC-f increases with the temperature, because the complex Poisson's ratio of the asphalt binder matrix increases with temperature. Moreover, Eqn 51 shows that the VSC increases with the complex Poisson's ratio; (3) the VSC-f increases with the filler content at the same temperature and crack length. This is due to that the VSC increases with the increase of the filler content; and (4) the

a. Evolution of the viscoelastic strengthening coefficient with fatigue cracks of the AM1

a. Calculation results of the viscoelastic strengthening coefficient with fatigue cracks of the AB, AM1 and AM2 at different temperatures

b. Evolution of the viscoelastic strengthening coefficient with fatigue cracks of the AM2

b. Shift model of the viscoelastic strengthening coefficient with fatigue cracks

Fig. 8. Evolution of the viscoelastic strengthening coefficient with fatigue cracks of the AM1 (AM1 = asphalt mastic with filler content of 10%) and AM2 (AM2 = asphalt mastic with filler content of 27%).
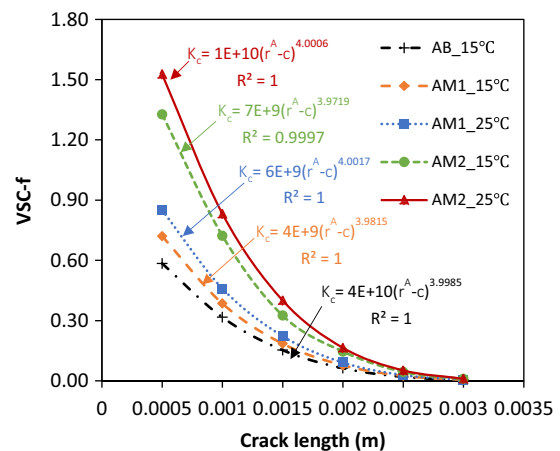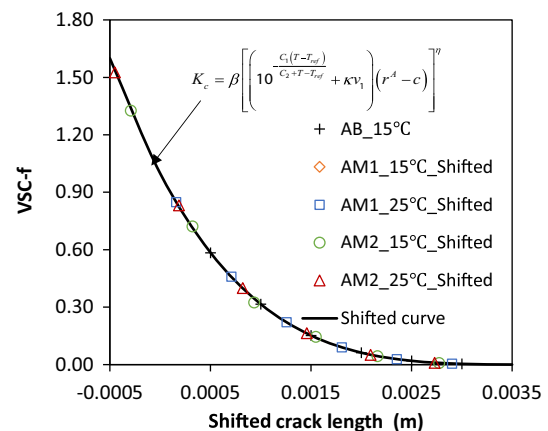
Fig. 9. Calculation results and shift model of the viscoelastic strengthening coefficient with fatigue cracks of the AB (AB = asphalt binder), AM1 (AM1 = asphalt mastic with filler content of 10%) and AM2 (AM2 = asphalt mastic with filler content of 27%) at different temperatures.
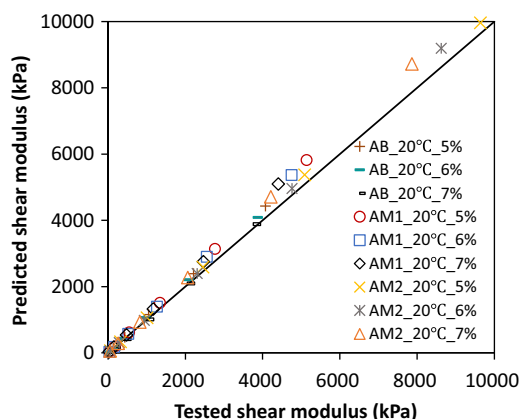
Fig. 10. Predicted and measured shear moduli of the AB (AB = asphalt binder), AM1 (AM1 = asphalt mastic with filler content of 10%) and AM2 (AM2 = asphalt mastic with filler content of 27%) at different strain levels and crack lengths of 20℃.

Table 5
Influence factors not covered in this study and their references.

Influence factors	References
Time-dependency	Traxler et al. [42]; Struik [43]; Bahia and Anderson [44]
Thermal stress	Saleh et al. [45]; Hiltunen et al. [46]; Velasquez et al. [47]
Strain rate	Li et al. [48]
Initial instability flow	Anderson et al. [49]

shifted model for the VSC-f can be established by taking the filler content into account, and Eqn 52 which considers the effect of the filler volumetric content and temperature can match the shifted VSC-f well.

Finally, to validate the VSC-f model coupled temperature, filler content and damage degree, the shear modulus of the viscoelastic asphalt-filler composite system at different strain levels and crack lengths are predicted based on Eqn 51 and 52. Fig. 10 shows predicted and measured shear moduli of the AB, AM1 and AM2 at different strain levels and crack lengths of 20℃. The results show that the model can well predict the shear modulus of the viscoelastic asphalt-filler composite system under the destructive fatigue load. It is indicated that the shifted model Eqn 52 and power function Eqn 51 can predict the shear modulus at different strain levels, temperatures, filler contents and damage degrees under the destructive condition.

6. Conclusions and future work

To address the challenge that accurately predicting mechanical properties for the viscoelastic asphalt composite materials, this study takes an asphalt-filler composite system as an example, and proposes a viscoelastic strengthening coefficient (VSC) model for the material at nondestructive condition (no fatigue cracks) and a viscoelastic strengthening coefficient with fatigue cracks (VSC-f) model at destructive condition (with fatigue cracks). This was achieved by using the Eshbely's equivalent inclusion theory and Mori-Tanaka approach. The established VSC model can reflect the strengthening effect of the filler inclusion on the asphalt binder matrix from the perspective of micromechanics. The established VSC-f model contains the reinforcement effect due to the filler inclusion and the weakening effect resulting from the fatigue cracks in the viscoelastic asphalt composite materials. Besides, the VSC and VSC-f contain the effect of complex Possion's ratio. The main findings of this study are listed below:

- Shear moduli of the asphalt-filler composite systems with filler volumetric contents of 10% and 27% are increased to 1.55 and 3.32 times that of the asphalt binder matrix at 10 Hz, 20℃.
- The VSC decreases with loading frequency or temperature, and increases with filler content. However, the VSC is independent of strain level.
- The predicted shear modulus results by the VSC model are in a good agreement with the tested shear modulus results at the low filler content, while they underestimate the shear modulus results at a high filler content. The predicted shear modulus results by a modified VSC model match the test shear modulus results at high filler content.
- The VSC-f model predictions matched with the test results under the destructive conditions. This model can predict shear modulus for the viscoelastic asphalt-filler composite system at different strain levels, temperatures, filler contents and damage levels.
- The VSC-f increases with the filler content, while decreases rapidly with fatigue crack length. The VSC-f is independent of strain level, and this is consistent with the VSC.

In this study, some factors affected the behavior of asphalt materials were not considered, such as time-dependency hardening of thermo-rheologically complex asphalt materials due to wax precipitation, thermal stress due to the temperature variations, strain rate and initial instability flow. These influence factors not covered in this study and their references are listed in Table 5.

These influence factors can be considered in future research. For example, the time dependency of the shift factors for the WLF relationship will be considered for some thermo-rheologically complex asphalt materials in the future. When studying the fatigue cracking of pavement structures in the future, the thermal stress should not be ignored (because of the temperature difference). In addition, more different asphalt binders, such as SBS asphalt binder, rubber asphalt binder, high-modulus asphalt binder and their composites mixed by different fillers, will be analyzed based on the micromechanics model developed in this study.

Declaration of Competing Interest

The authors declare that they have no known competing financial interests or personal relationships that could have appeared to influence the work reported in this paper.

Acknowledgements

Appendix A

It is assumed that the apparent shear stress, strain and disturbed stress, strain and stress, strain difference of the asphalt binder matrix and viscoelastic asphalt-filler composite system linearly increase from the loading center to the edge of the specimen under the controlled-strain cyclic shear load, and the filler particles are uniformly distributed in the asphalt binder matrix. Therefore, the volumetric integrals of these stresses and strains have the same operation. Taking the apparent shear strain of asphalt binder matrix as an example, the volumetric integral of the apparent

shear strain of the viscoelastic asphalt-filler composite system can be obtained based on Eqn 19:

$$\frac{1}{V}\iiint\limits_V \bar{\varepsilon}_{12}^{0A}(t_0,r)dV = \frac{1}{\pi(r^A)^2 h}2\pi h\int_0^{r^A}\frac{r^2}{r^A}\bar{\varepsilon}_{12}^{0A}(t_0,r^A)dr$$

$$= \frac{2}{3}\bar{\varepsilon}_{12}^{0A}(t_0,r^A) = \frac{2}{3}\bar{\varepsilon}_{12}^{0} \quad\quad (A.1)$$

where $\bar{\varepsilon}_{12}^{0A}(t_0,r)$ is apparent shear strain of the asphalt binder matrix at loading time t_0, any radius r in the Laplace domain; h is height of the asphalt binder matrix specimen. For the sake of simplicity, the $\bar{\varepsilon}_{12}^{0A}(t_0,r)$ is denoted as $\bar{\varepsilon}_{12}^{0}$, the same definition is applied to the stresses and strains listed below.

Therefore, in the Laplace domain, the statistically uniform stress $\left\langle \bar{\sigma}_{12}^{eA} \right\rangle$ of the viscoelastic asphalt-filler composite system is shown as follows:

$$\left\langle \bar{\sigma}_{12}^{eA} \right\rangle = \frac{1}{V}\iint\limits_V \bar{\sigma}_{12}^{eA}(t_0,r)dV$$

$$= \frac{2}{3}v_0\bar{C}_{1212}^{0}\left(\bar{\varepsilon}_{12}^{0}+\bar{\varepsilon}_{12}^{d}\right) + \frac{2}{3}v_1\bar{C}_{1212}^{0}\left(\bar{\varepsilon}_{12}^{0}+\bar{\varepsilon}_{12}^{d}+\bar{\varepsilon'}_{12}^{*}-\bar{\varepsilon}_{ij}^{*}\right)$$

$$= \frac{2}{3}\bar{C}_{1212}^{0}\left[(1-v_1)\left(\bar{\varepsilon}_{12}^{0}+\bar{\varepsilon}_{12}^{d}\right) + v_1\left(\bar{\varepsilon}_{12}^{0}+\bar{\varepsilon}_{12}^{d}+\bar{\varepsilon'}_{12}^{*}-\bar{\varepsilon}_{ij}^{*}\right)\right]$$

$$= \frac{2}{3}\bar{C}_{1212}^{0}\left(\bar{\varepsilon}_{12}^{0}+\bar{\varepsilon}_{12}^{d}+v_1\bar{\varepsilon'}_{12}^{*}-v_1\bar{\varepsilon}_{ij}^{*}\right)$$

$$= \frac{2}{3}\bar{C}_{1212}^{0}\left(\bar{\varepsilon}_{12}^{0}-v_1(S_{ijkl}-I_{ijkl})\bar{\varepsilon}_{kl}^{*}+v_1 S_{ijkl}\bar{\varepsilon}_{kl}^{*}-v_1\bar{\varepsilon}_{ij}^{*}\right)$$

$$= \frac{2}{3}\bar{C}_{1212}^{0}\left(\bar{\varepsilon}_{12}^{0}+v_1 I_{ijkl}\bar{\varepsilon}_{kl}^{*}-v_1\bar{\varepsilon}_{ij}^{*}\right)$$

$$= \frac{2}{3}\bar{C}_{1212}^{0}\bar{\varepsilon}_{12}^{0} \quad\quad (A.2)$$

Then, the statistically uniform strain can be calculated by:

$$\left\langle \bar{\varepsilon}_{12}^{eA} \right\rangle = \frac{1}{V}\iint\limits_V \bar{\varepsilon}_{12}^{eA}dV$$

$$= \frac{2}{3}\left[v_0\left(\bar{\varepsilon}_{12}^{0}+\bar{\varepsilon}_{12}^{d}\right)+v_1\left(\bar{\varepsilon}_{12}^{0}+\bar{\varepsilon}_{12}^{d}+\bar{\varepsilon'}_{12}^{*}\right)\right]$$

$$= \frac{2}{3}\left[(1-v_1)\left(\bar{\varepsilon}_{12}^{0}+\bar{\varepsilon}_{12}^{d}\right)+v_1\left(\bar{\varepsilon}_{12}^{0}+\bar{\varepsilon}_{12}^{d}+\bar{\varepsilon'}_{12}^{*}\right)\right]$$

$$= \frac{2}{3}\left[\bar{\varepsilon}_{12}^{0}+\bar{\varepsilon}_{12}^{d}+v_1\bar{\varepsilon'}_{12}^{*}\right]$$

$$= \frac{2}{3}\left[\bar{\varepsilon}_{12}^{0}-v_1(S_{1212}-I_{1212})\bar{\varepsilon}_{12}^{*}+v_1 S_{1212}\bar{\varepsilon}_{12}^{*}\right]$$

$$= \frac{2}{3}\left[\bar{\varepsilon}_{12}^{0}+v_1\bar{\varepsilon}_{12}^{*}\right]$$

$$= \frac{2}{3}\left\{v_1\left[\bar{G}^0-\bar{G}^1\right]\left[\left(\bar{G}^1-\bar{G}^0\right)(v_2 S_{1212}+v_1 I_{1212})-\bar{G}^0\right]^{-1}+I_{1212}\right\}\bar{\varepsilon}_{12}^{0A}$$

$$(A.3)$$

In addition, $\bar{\lambda}^0 << \bar{\lambda}^1$, $\bar{G}^0 << \bar{G}^1$, Eqn A.3 can be simplified as below:

$$\left\langle \bar{\varepsilon}_{12}^{eA} \right\rangle = \frac{2}{3}\left\{-v_1[(v_0 S_{1212}+v_1 I_{1212})]^{-1}+I_{1212}\right\}\bar{\varepsilon}_{12}^{0} \quad\quad (A.4)$$

References

[1] X. Luo, B. Birgisson, R.L. Lytton, Kinetics of healing of asphalt mixtures, J. Cleaner Prod. 252 (2020) 119790.

[2] X. Luo, H. Li, Y. Deng, Y. Zhang, Energy-Based kinetics approach for coupled viscoplasticity and viscofracture of asphalt mixtures, J. Eng. Mech. 146 (9) (2020) 04020100.

[3] E.L. Omairey, F. Gu, Y. Zhang, An equation-based multiphysics modelling framework for oxidative ageing of asphalt pavements, J. Cleaner Prod. 280 (2021) 124401.

[4] M.W. Witczak, O.A. Fonseca, Revised predictive model for dynamic (complex) modulus of asphalt mixtures, Transp. Res. Rec. 1540 (1) (1996) 15–23.

[5] J. Bari, M. Witczak, Development of a New Revised Version of the Witczak E* Predictive Model for Hot Mix Asphalt Mixtures (With Discussion), J. Assoc. Asphalt Paving Technol. 75 (2006).

[6] F. Bonnaure, G. Gest, A. Gravois, P. Uge, A new method of predicting the stiffness of asphalt paving mixtures, Proc. Assoc. Asphalt Paving Technol. 46 (1977) (1977) 61–100.

[7] M.H. Sadd, Q. Dai, V. Parameswaran, A. Shukla, Microstructural simulation of asphalt materials: modeling and experimental studies, J. Mater. Civ. Eng. 16 (2) (2004) 107–115.

[8] Y. Zhang, T. Ma, M. Ling, D. Zhang, X. Huang, Predicting dynamic shear modulus of asphalt mastics using discretized-element simulation and reinforcement mechanisms, J. Mater. Civ. Eng. 31 (8) (2019) 04019163.

[9] H. Wang, W. Huang, J. Cheng, G. Ye, Mesoscopic creep mechanism of asphalt mixture based on discrete element method, Constr. Build. Mater. 272 (2021) 121932.

[10] P. Karki, Y.R. Kim, D.N. Little, Dynamic modulus prediction of asphalt concrete mixtures through computational micromechanics, Transp. Res. Rec. 2507 (1) (2015) 1–9.

[11] J. Chen, H. Wang, H. Dan, Y. Xie, Random modeling of three-dimensional heterogeneous microstructure of asphalt concrete for mechanical analysis, J. Eng. Mech. 144 (9) (2018) 04018083.

[12] J. Li, J. Zhang, G. Qian, J. Zheng, Y. Zhang, Three-dimensional simulation of aggregate and asphalt mixture using parameterized shape and size gradation, J. Mater. Civ. Eng. 31 (3) (2019) 04019004.

[13] X. Ding, T. Ma, W. Zhang, D. Zhang, T. Yin, Effects by property homogeneity of aggregate skeleton on creep performance of asphalt concrete, Constr. Build. Mater. 171 (2018) 205–213.

[14] K. Anupam, S.K. Srirangam, A. Varveri, C. Kasbergen, A. Scarpas, Microstructural analysis of porous asphalt concrete mix subjected to rolling truck tire loads, Transp. Res. Rec. 2575 (1) (2016) 113–122.

[15] J. Chen, H. Wang, L. Li, Virtual testing of asphalt mixture with two-dimensional and three-dimensional random aggregate structures, Int. J. Pavement Eng. 18 (9) (2017) 824–836.

[16] M. Salemi, H. Wang, Image-aided random aggregate packing for computational modeling of asphalt concrete microstructure, Constr. Build. Mater. 177 (2018) 467–476.

[17] Eshelby, J. D. (1957). The determination of the elastic field of an ellipsoidal inclusion, and related problems. Proceedings of the royal society of London. Series A. Mathematical and physical sciences, 241(1226), 376-396.

[18] J.D. Eshelby, The elastic field outside an ellipsoidal inclusion, Proc. R. Soc. Lond. A 252 (1271) (1959) 561–569.

[19] R. Hill, A self-consistent mechanics of composite materials, J. Mech. Phys. Solids 13 (4) (1965) 213–222.

[20] R.M. Christensen, K.H. Lo, Solutions for effective shear properties in three phase sphere and cylinder models, J. Mech. Phys. Solids 27 (4) (1979) 315–330.

[21] T. Mori, K. Tanaka, Average stress in matrix and average elastic energy of materials with misfitting inclusions, Acta Metall. 21 (5) (1973) 571–574.

[22] R. Roscoe, The viscosity of suspensions of rigid spheres, Br. J. Appl. Phys. 3 (8) (1952) 267.

[23] R. McLaughlin, A study of the differential scheme for composite materials, Int. J. Eng. Sci. 15 (4) (1977) 237–244.

[24] J.W. Ju, T.M. Chen, Micromechanics and effective moduli of elastic composites containing randomly dispersed ellipsoidal inhomogeneities, Acta Mech. 103 (1–4) (1994) 103–121.

[25] J. Zhang, Z. Fan, H. Wang, W. Sun, J. Pei, D. Wang, Prediction of dynamic modulus of asphalt mixture using micromechanical method with radial distribution functions, Mater. Struct. 52 (2) (2019) 49.

[26] C. Peng, J. Feng, S. Feiting, Z. Changjun, F. Decheng, Modified two-phase micromechanical model and generalized self-consistent model for predicting dynamic modulus of asphalt concrete, Constr. Build. Mater. 201 (2019) 33–41.

[27] R. Luo, R.L. Lytton, Self-consistent micromechanics models of an asphalt mixture, J. Mater. Civ. Eng. 23 (1) (2011) 49–55.

[28] China, M. (2011). Standard Test Methods of Bitumen and Bituminous Mixtures for Highway Engineering: JTG E20-2011.

[29] T. Mura, Micromechanics of Defects in Solids, Martinus Nijhoff Publ, 1987.

[30] X. Huang, H. Li, Y. Zhang, Micromechanics analysis of viscoelasticity for asphalt mixtures considering influences of coarse aggregates and voids, Journal of South China University of Technology (Natural Science) 37 (7) (2009) 31.

[31] A. Roatta, R.E. Bolmaro, An Eshelby inclusion-based model for the study of stresses and plastic strain localization in metal matrix composites I: General formulation and its application to round particles, Mater. Sci. Eng., A 229 (1–2) (1997) 182–191.

[32] P.A. Cundall, Computer simulations of dense sphere assemblies, Studies in Applied Mechanics 20 (1988) 113–123.

[33] Y. Zhang, R. Luo, R.L. Lytton, Anisotropic characterization of crack growth in the tertiary flow of asphalt mixtures in compression, J. Eng. Mech. 140 (6) (2014) 04014032.

[34] H.D. Benedetto, B. Delaporte, C. Sauzéat, Three-dimensional linear behavior of bituminous materials: experiments and modeling, Int. J. Geomech. 7 (2) (2007) 149–157.

[35] Pellinen, T. K., Witczak, M. W., and Bonaquist, R. F. (2002). "Asphalt mix master curve construction using sigmoidal fitting function with nonlinear least squares optimization." Proc., Pavement Mechanics Symp. at the 15th ASCE Engineering Mechanics Division Conf., ASCE, Reston, VA.

[36] V.K. Shante, S. Kirkpatrick, An introduction to percolation theory, Adv. Phys. 20 (85) (1971) 325–357.

[37] N.D. Alberola, P. Mele, Viscoelasticity of polymers filled by rigid or soft particles: theory and experiment, Polym. Compos. 17 (5) (1996) 751–759.

[38] H. Li, X. Luo, W. Yan, Y. Zhang, Energy-Based Mechanistic Approach for Crack Growth Characterization of Asphalt Binder, Mech. Mater. 103462 (2020).

[39] Y. Zhang, Y. Gao, Predicting crack growth in viscoelastic bitumen under a rotational shear fatigue load, Road Materials and Pavement Design (2019) 1–20.

[40] H. Li, X. Luo, Y. Zhang, A kinetics-based model of fatigue crack growth rate in bituminous material, Int. J. Fatigue 148 (2021) 106185.

[41] L. Li, Y. Gao, Y. Zhang, Crack length based healing characterisation of bitumen at different levels of cracking damage, J. Cleaner Prod. 258 (2020) 120709.

[42] Traxler R.N. & Schweyer H.E. (1936). Increase in viscosity of asphalts with time. Proc. Thirty-Ninth Annual Meeting, American Society for Testing Materials 36(I1): 544- 550.Atlantic City, New Jersey, United States.

[43] Struik, L. C. E. (1977). Physical aging in amorphous polymers and other materials.

[44] Bahia, H.U. & Anderson, D.A. (1991). Isothermal lowtemperature physical hardening of asphalt. Proc. Intern.Symp. Chemistry of Bitumens 1: 114-147, Rome, Italy.

[45] N.F. Saleh, B. Keshavarzi, F.Y. Rad, D. Mocelin, M. Elwardany, C. Castorena, Y.R. Kim, Effects of aging on asphalt mixture and pavement performance, Constr. Build. Mater. 258 (2020) 120309.

[46] D.R. Hiltunen, R. Roque, A Mechanics-Based Prediction Model For Thermal Cracking Of Asphaltic CoNCrete Pavements, J. Assoc. Asphalt Paving Technol. 63 (1994) 81–117.

[47] R. Velasquez, H. Bahia, Critical factors affecting thermal cracking of asphalt pavements: towards a comprehensive specification, Road Materials and Pavement Design 14 (sup1) (2013) 187–200.

[48] Q. Li, X. Ma, F. Ni, G. Li, Characterization of strain rate and temperature-dependent shear properties of asphalt mixtures, J. Test. Eval. 43 (5) (2015) 20140056.

[49] D. Anderson, Y. Hir, M. Marasteanu, J.P. Planche, D. Martin, G. Gauthier, Evaluation of fatigue criteria for asphalt binders, Transportation Research Record Journal of the Transportation Research Board 1766 (2001) 48–56.

[50] H. Li, X. Luo, Y. Zhang, Pseudo Energy-based Kinetic Characterization of Fatigue in Asphalt Binders, China Journal of Highway and Transport 33 (10) (2020) 115–124, https://doi.org/10.19721/j.cnki.1001-7372.2020.10.006.

[51] H. Li, X. Luo, Y. Zhang, R. Xu, Stochastic Fatigue Damage in Viscoelastic Materials using Probabilistic Pseudo J-Integral Paris' Law, Engineering Fracture Mechanics 245 (1) (2021), https://doi.org/10.1016/j.engfracmech.2021.107566 107566.

[52] F. Gu, R. Moraes, C. Chen, F. Yin, D. Watson, A. Taylor, Effects of Additional Antistrip Additives on Durability and Moisture Susceptibility of Granite-Based Open-Graded Friction Course, Journal of Materials in Civil Engineering 33 (9) (2021), https://doi.org/10.1061/(ASCE)MT.1943-5533.0003862 04021245.